RESEARCH ARTICLE | JULY 29 2008

Slab waveguides and nanoscale patterning of pulsed laser-deposited $Ge_{0.2}Se_{0.8}$ chalcogenide films

W. C. Liu; G. Hoffman; W. Zhou; R. M. Reano; P. Boolchand; R. Sooryakumar

Appl. Phys. Lett. 93, 041107 (2008)
https://doi.org/10.1063/1.2965124

Slab waveguides and nanoscale patterning of pulsed laser-deposited $Ge_{0.2}Se_{0.8}$ chalcogenide films

W. C. Liu,[1,3] G. Hoffman,[2] W. Zhou,[1] R. M. Reano,[2] P. Boolchand,[4] and R. Sooryakumar[1,a)]
[1]*Department of Physics, The Ohio State University, Columbus, Ohio 43210, USA*
[2]*Department of Electrical and Computer Engineering The Ohio State University, Columbus, Ohio 43210, USA*
[3]*Department of Applied Physics, The Hong Kong Polytechnic University, Hung Hom, Kowloon 852, Hong Kong*
[4]*Department of Electrical, Computer Engineering and Computer Science, University of Cincinnati, Cincinnati, Ohio 45221, USA*

(Received 12 June 2008; accepted 30 June 2008; published online 29 July 2008)

Planar slab waveguides were fabricated by pulsed laser deposition from Ge_xSe_{1-x} glass compounds with composition ($x \sim 0.2$) that lies very close to the floppy to rigid stiffness transition. These high quality active structures, which were deposited on SiO_2 cladding layers above silicon substrates, support several transverse-electric (TE) modes, and a loss of 0.24 dB/cm for the TE_0 mode was measured at 632.8 nm wavelength. The ability to exploit electron beam writing at these special Ge in Se compositions to create nanoscale surface motifs are promising advances to create unique miniature optical processing devices. © *2008 American Institute of Physics*.
[DOI: 10.1063/1.2965124]

Glasses are varied and complex materials[1,2] with an assembly of interconnected structural units whose relaxation has been arrested to varying degrees. As the number of these cross-links within a covalent network increases by compositional tuning, these systems steadily evolve from being underconstrained (floppy) to an overconstrained (rigid) solid.[3,4] This rigidity transformation has generated wide interest[5–10] because the connectivity (or average coordination) is not only a good parameter to describe many thermodynamic properties of the glass transition but residual stresses are also minimized in its immediate vicinity.[11] The near absence of stress in the network has borne out new phenomena including the large-scale photoreversible glass state in bulk chalcogenide (Ge_xSe_{1-x}, for $x \sim 0.2$) samples.[12] Moreover, we find that close to this unique composition in the same Ge in Se system, structural motifs corresponding to surface reliefs and trenches can be readily created when the amorphous films are exposed to electron beams.

In this paper we present results on the fabrication and slab waveguide properties of Ge_xSe_{1-x} films that lie at the mean-field rigidity percolation threshold. High quality homogeneous films with smooth surfaces and low-loss waveguiding properties were grown by pulsed laser deposition.[13] We show the support of seven transverse-electric (TE) modes. Maskless direct-write e-beam contours are used to induce reliefs and trenches that can be controlled at the nanometer range by scaling the electron dosage. Thus, when combined with (a) characteristic low-phonon energy and visible to mid-infrared transparency, (b) high refractive indices that lead to high contrast small bending radius waveguiding structures, and (c) ultrafast photoresponse times,[14] the ability to directly write ultrafine structural features make the Ge_xSe_{1-x} system as promising candidates for developing advanced chip-scale photonic devices.

Bulk $Ge_{0.2}Se_{0.8}$ target samples were synthesized from the elements in evacuated quartz tubes, followed by quenching of the melt. Films of thicknesses ranging from 400 nm to several microns were produced by ablating the rotating targets in $\sim 10^{-5}$ Torr vacuum using a KrF excimer laser (Lambda Physik model 305i) operating at $\lambda = 248$ nm and a constant output energy of 300 mJ/pulse. The pulse duration was 30 ns and the repetition rate was 5 Hz. The films were deposited onto 4 μm thick thermally oxidized Si substrates. The SiO_2 film ($n = 1.46$) serves as the slab waveguide cladding.

The chemical composition and homogeneity of the films were monitored through Raman scattering. The principal Raman features observed are modes at 195, 215, and 260 cm^{-1} [Figs. 1(a)–1(d)] arising respectively from the $GeSe_{4/2}$ corner-sharing and edge-sharing $GeSe_{4/2}$ tetrahedra and Se_n-chain vibrations.[7] These findings are in excellent agreement with the spectra recorded from the bulk glasses[7] of the same composition [Fig. 1(e)]. The essentially identical Raman spectra measured from widely separated (approximately centimeters) regions in the film confirm their excellent compositional homogeneity and validate the ability to simultaneously deposit the volatile and nonvolatile parts of the target material.

The optical properties of the $Ge_{0.2}Se_{0.8}$ slab waveguides were measured using the prism-coupling technique (Metricon, USA).[15,16] The method allows for the determination of the film's refractive index, thickness, and the propagation constants of each of the film's light guiding modes. Figure 2(a) reveals seven TE modes in a 1.05 μm thick $Ge_{0.2}Se_{0.8}$ film. Losses incurred are determined by measuring, down the length of the guide, the light intensity scattered from the surface. Since this intensity is proportional to the light that remains within the waveguide, the best exponential fit to the resulting intensity versus distance curve yields the loss in dB/cm [Fig. 2(b)]. The predominant source of loss in planar optical waveguides is scattering from the surface. For example, the measured low-loss value of 0.24 dB/cm [Fig.

a)Electronic mail: soory@mps.ohio-state.edu.

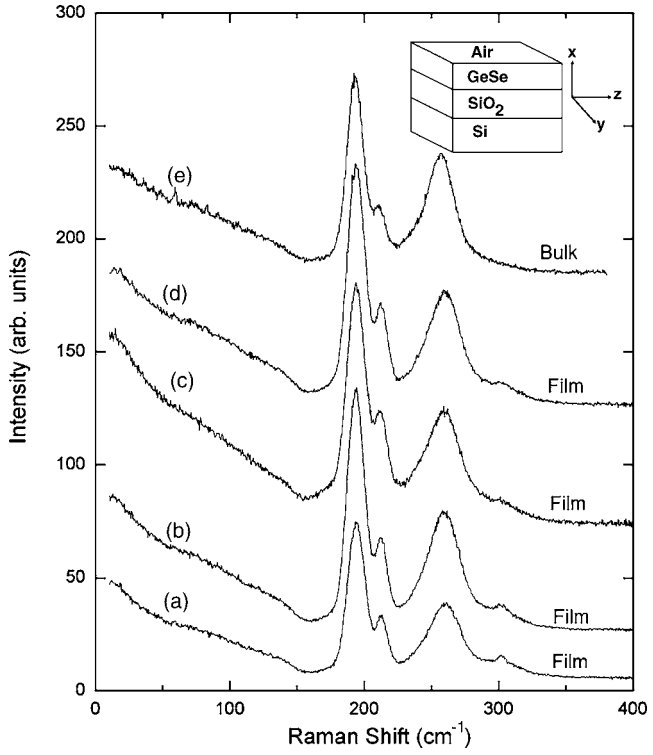

FIG. 1. Raman spectra recorded at room temperature from a $Ge_{0.2}Se_{0.8}$ film deposited on a SiO_2/Si substrate. The data were taken with 50 mW of 647 nm laser power. Spectra (a)–(d) were from various locations on the film. For comparison, spectrum (e) was recorded from a bulk $Ge_{0.2}Se_{0.8}$ sample.

2(b)] is especially significant wherein the waveguide supports many modes since the higher order modes scatter more strongly at the surface.

The waveguide geometry we utilize is the four layer (air/$GeSe_4$/SiO_2/Si) structure shown in Fig. 1. Since all layers are planar, homogeneous, and isotropic in the y and z directions we consider propagation in the z direction and ignore variations in the y direction. The TE modes are specified by solutions of Maxwell's equations in the layered media for the y component of the electric field E_y given by $E_y(x,z,t)=E_y(x)e^{-i(\beta z-\omega t)}$, where β is the complex propagation constant. In our case, since the SiO_2 (layer 3, $n_3=1.46$) is relatively thick (4 μm) and provides sufficiently strong confinement to the chalcogenide film (layer 2; $n_2=2.44$), fields at the cladding layer-Si substrate interface are very small. Thus we neglect the effects of the Si substrate (layer 4) and seek wave equation solutions, where $n_3<\mathrm{Re}[n_e]<n_2$, for $n_3>n_1$ (=1, air). The dispersion diagrams for the TE modes are generated by numerically solving the resulting transcendental equation[17]

$$\tan(ht)=\frac{h(p+q)}{h^2-pq},$$

where $p=(\beta^2-k^2n_3^2)^{1/2}$, $h=(k^2n_2^2-\beta^2)^{1/2}$, and $q=(\beta^2-k^2n_1^2)^{1/2}$.

Solutions are found by iterating the index n_e between n_2 and n_3; the resulting dispersion is illustrated by the solid curves in Fig. 2(c) for a waveguide with an active chalco-

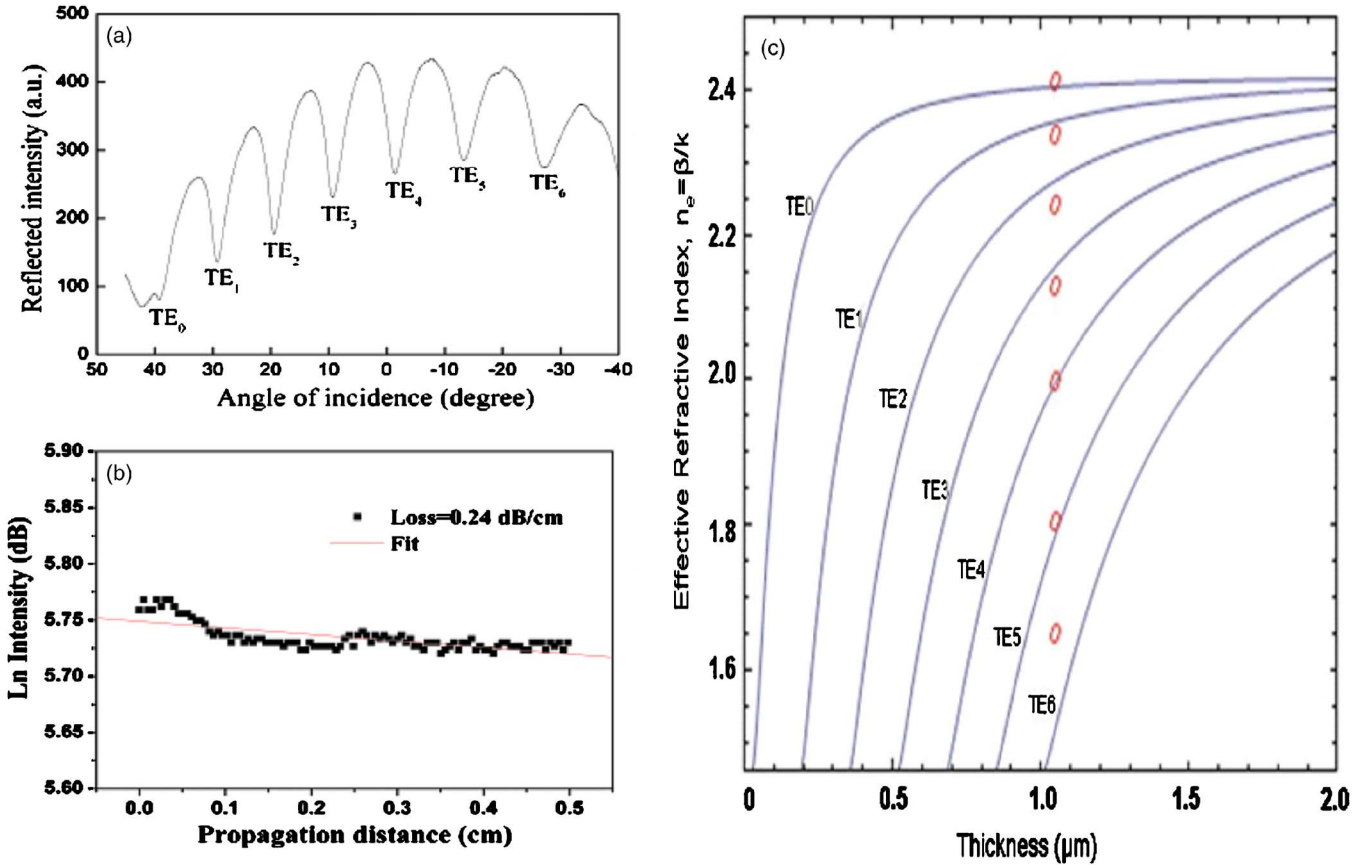

FIG. 2. (Color online) (a) Excited TE mode spectra for the air/$Ge_{0.2}Se_{0.8}$/SiO_2 slab waveguide on a Si substrate. The measurements were recorded using a Metricon 2010 prism-coupling technique. Up to seven TE_m modes are supported in this structure with a 1.05 μm active $Ge_{0.2}Se_{0.8}$ chalcogenide layer. (b) Optical loss measurements for the TE_0 mode of the same waveguide. (c) Dispersion diagrams for the above air/$Ge_{0.2}Se_{0.8}$/SiO_2 slab waveguide. The individual data (open circles) are experimental values obtained using the prism-coupling method.

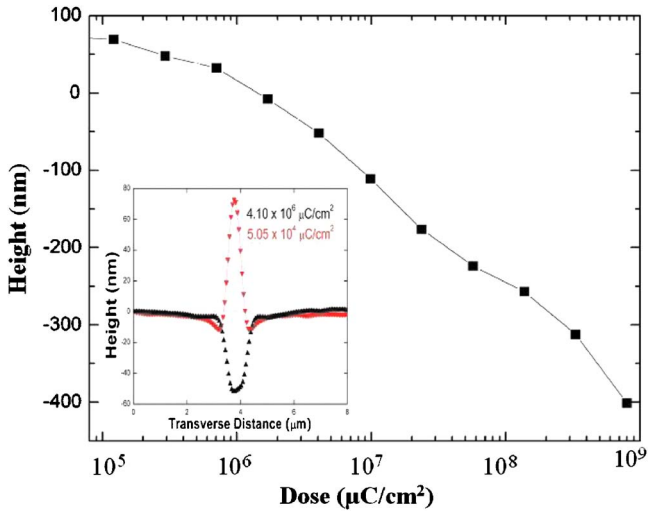

FIG. 3. (Color online) AFM measurements of relief height, relative to the original film surface, vs electron beam dose. The inset shows AFM measurements of cross-sectional profiles of electron beam induced reliefs revealing the presence of a transition dosage between trenches and reliefs.

genide layer thickness of 1.05 μm. Experimental values for the equivalent index $n_e=\beta/k$ obtained are plotted in Fig. 2(c) as open circles. Good general agreement is achieved between the measured TE_m modes [Fig. 2(a)] and the numerical solutions of the three-layer mode equations. The deviation evident for the TE_6 mode is likely a result of being near the cutoff.

In order to further develop these planar slab chalcogenide layers into prospective nanoscale waveguides with in-plane confinement, we investigated the use of electron beam lithography to construct surface configurations with the high resolution offered by e-beam writing.[18,19] In selecting a special Ge_xSe_{1-x} glass composition ($x=0.2$) corresponding to its rigidity transition and stress-free nature, we observe (Fig. 3) that tuning the electron current dose creates a nanoscale surface mound or relief profile. The inset in Fig. 3 is an atomic force microscope (AFM) image showing the cross-sectional profile for a given electron beam dose. At larger dosage, the reliefs transform to trenches that are accompanied with slightly raised edges that slowly taper from the center of the trench. In the illustrative example (Fig. 3) showing the relief height versus electron beam dosage, a net variation of ~500 nm is evident between trench depth and mound height. The most likely origin for mound or trench formation is competing e-beam induced expansion due to bond breakage and Coulombic repulsion effects. At higher dosage, excess charging causes the lost material in the trench to be moved and compensated by the expansion of the material around the trench. Both of these types of deformations could be used in optical gratings, waveguides, and waveguide-cavity coupled structures. This finding opens up new directions in the development of planar optical chalcogenide waveguides that have several advantages over current techniques that rely on photodarkening, photodoping, photolithography, and ionimplantation.[14,20–24] These advantages include maskless e-beam writing that greatly simplifies fabrication procedure while offering nanoscale dimensional control as well as formation of inherent rib-waveguide structures which are less susceptible to surface roughness scattering loss (dominant loss source in planar optical waveguides).

In conclusion, we have demonstrated that $Ge_{0.20}Se_{0.80}$ optical waveguides with low attenuation, ~0.24 dB/cm, for TE_m modes can be deposited by pulsed laser deposition on silicon wafers with SiO_2 buffer layer. Our findings show that the Ge–Se chalcogenide system can be readily integrated into existing silica-on-silicon planar waveguide technology and that, at least for compositions in the neighborhood of the stress-free stiffness transition, electron beams can be effectively used to create surface patterns. These findings are promising not only for optical waveguide applications and development of chip-scale photonic devices but also for the continued convergence of silicon based electronics and photonics.

We thank I. Hetel and T. R. Lemberger for assistance with the PLD system and P. Chen for recording the Raman data. This work was supported by the NSF under Grants Nos. ECCS 0701686 and DMR 0456472.

[1] R. Zallen, *The Physics of Amorphous Solids* (Wiley, New York, 1983).
[2] P. Boolchand, G. Lucovsky, J. C. Phillips, and M. F. Thorpe, Philos. Mag. **85**, 3823 (2005).
[3] J. C. Phillips, J. Non-Cryst. Solids **34**, 153 (1979).
[4] M. F. Thorpe, J. Non-Cryst. Solids **57**, 355 (1983).
[5] *Rigidity Theory and Applications*, edited by M. F. Thorpe and P. M. Duxbury (Kluwer Academic/Plenum Publishers, New York, 1999).
[6] H. He and M. F. Thorpe, Phys. Rev. Lett. **54**, 2107 (1985).
[7] X. Feng, W. J. Bresser, and P. Boolchand, Phys. Rev. Lett. **78**, 4422 (1997).
[8] J. C. Phillips, in *Rigidity Theory and Applications*, edited by M. F. Thorpe and P. M. Duxbury (Kluwer Academic/Plenum Publishers, New York, 1999), p. 155.
[9] B. A. Weinstein, R. Zallen, and M. L. Slade, Phys. Rev. B **25**, 781 (1982); **24**, 4652 (1981).
[10] P. Boolchand, X. Feng, D. Selvanathan, and W. Bresser, in *Rigidity Theory and Applications*, edited by M. F. Thorpe and P. M. Duxbury (Kluwer Academic/Plenum Publishers, New York, 1999), p. 279, and references therein.
[11] F. Wang, S. Mamedov, P. Boolchand, B. Goodman, and M. Chandrasekhar, Phys. Rev. B **71**, 174201 (2005).
[12] J. Gump, I. Finkler, H. Xia, R. Sooryakumar, W. J. Bresser, and P. Boolchand, Phys. Rev. Lett. **92**, 245501 (2004).
[13] M. Frumar, B. Frumarova, P. Nemec, T. Wagner, J. Jedelsky, and M. Hrdlicka, J. Non-Cryst. Solids **352**, 544 (2006).
[14] S. Spalter, H. Y. Hwang, I. Zimmerman, G. Lez, T. Katsufuji, S.-W. Cheong, and R. E. Slusher, Opt. Lett. **27**, 363 (2002).
[15] R. Ulrich and R. Torge, Appl. Opt. **12**, 2901 (1973).
[16] W. C. Liu, C. L. Mak, and K. H. Wong, J. Phys. D: Appl. Phys. **40**, 749 (2007).
[17] R. G. Hunsperger, *Integrated Optics: Theory and Technology*, (Springer, Berlin, 1991).
[18] K. Tanaka, Appl. Phys. Lett. **70**, 261 (1997).
[19] J. Romero, A. Frizgerald, and K. Mietzsch, J. Appl. Phys. **91**, 9572 (2002).
[20] A. Zakery, Y. Ruan, A. V. Rode, M. Samoc, and B. Luther-Davies, J. Opt. Soc. Am. B **20**, 1844 (2003).
[21] M. Frumar and T. Wagner, Curr. Opin. Solid State Mater. Sci. **7**, 117 (2003).
[22] J.-F. Viens, C. Meneghini, A. Villeneuve, T. V. Galstian, E. J. Knystautas, M. A. Duguay, K. A. Richardson, and T. Cardinal, J. Lightwave Technol. **17**, 1184 (1999).
[23] S. Ramachandran and S. G. Bishop, Appl. Phys. Lett. **74**, 13 (1999).
[24] C. Gmachl, H. Y. Hwang, R. Paiella, D. L. Sivco, J. N. Baillargeon, F. Capasso, and A. Y. Cho, IEEE Photonics Technol. Lett. **13**, 182 (2001).